Review | Received 28 July 2024; Accepted 11 November 2024; Published 16 November 2024
https://doi.org/10.55092/neuroelectronics20240002

A review of wireless intra-body communication for neural implants

Chuer Lin[1,2], Shengqi Zhu[1], Cheng Han[1,2], Shan Yu[1], Zhiwei Zhang[1,*], and Jingna Mao[1,*]

[1]Institute of Automation, Chinese Academy of Sciences, Beijing, China
[2]School of Future Technology, University of Chinese Academy of Sciences, Beijing, China

* Correspondence authors; E-mail: zhiwei.zhang@ia.ac.cn, jingna.mao@ia.ac.cn.

Abstract: Neural interfaces have played an increasingly significant part in people's lives. A mm-scale fully-implanted neural system-on-a-chip is required for long-term bio-compatible recording in applications such as fundamental neuroscience research, neural prosthesis, and neurological disease diagnosis. This paper aims to survey and discuss the current wireless intra-body communication methods used in neural implants, including far-field radio frequency, near-field inductive coupling, ultrasonic, near-infrared, capacitive body coupling, and galvanic body coupling communication. Starting with the discussion of communication requirements, the performance of each approach is evaluated in terms of mechanism, trade-offs, characteristics, and tissue safety. From the viewpoint of wireless communication, we present a detailed analysis and comparison of neural implants that employ different data telemetry technologies. After identifying the challenges of neural implants, several optimizations are summarized.

Keywords: neural implant; brain-computer interface; neuronal recording system; biomedical implant; wireless communication; biomedical communication; intra-body communication

1. Introduction

In recent years, neural interfaces have played an increasingly important role in people's lives. Compared with non-invasive approaches, invasive neural devices can capture signals with greater resolution and signal-to-noise ratio (SNR). Implanted interfaces are therefore more effective in fundamental neuroscience research [1], neural prostheses [2], and the diagnosis and intervention of neurological diseases [3]. Early neural recording systems utilized cables to connect implanted electrodes and external signal processing equipment for power and data transfer [4, 5] . Such a wired connection increases the risk of wound infection, restricts animal movement, and causes additional noise interference. To eliminate physical tethers, wireless power and data technologies are then integrated onto printed circuit boards (PCBs) and linked to implanted neural probes to form head-mounted devices [6]. Though animals can move freely, the relatively heavy weight of the neural interface generates stress and may harm their physical and mental health. To minimize risks, a mm-scale fully-implanted neural interfacing system-on-a-chip (SoC) is required for long-term bio-compatible recording.

The previous reviews about implantable devices, listed in Table. 1, lack thorough investigation on the communication methods of neural implants. Several aspects of neural interfaces have been investigated, such as high-density electrodes [7], signal processing techniques [8], battery-free technologies [9], SoC designs [10], and the application of multimodal electrical neuromudulation [11]. Furthermore, there are some comprehensive surveys of biomedical implants [12–15] that cover wireless communication methods. However, path loss or tissue safety of various data transmission techniques are not studied in these papers. Additionally, several

Table 1. Related Works

Year	Ref.	Type	Content & Style
2024	[11]	Review	Implantable Neural Interfaces for Multimodal Electrical Neuromodulation
2024	[17]	Survey	Near-field wireless communication and power transfer for biomedical implants
2024	[9]	Review	Energy transfer mechanisms for neural implants
2024	[7]	Review	High-density implantable neural electrodes and chips
2023	[8]	Magazine	Signal processing of brain-computer interfaces
2023	[10]	Magazine	Wireless neural interface SoC designs
2023	[12]	Review	Wireless, batteryless, implantable electronics for physiological monitoring
2023	[13]	Review	Miniature battery-free bioelectronics
2020	[14]	Review	Four generations of electronic neural interfaces
2020	[15]	Review	Electrical neural interface
2019	[16]	Survey	Intra-body communication technologies

promising intra-body telemetry approaches are not analyzed, including near-infrared [16] and human body communication [17]. Therefore, this survey systematically investigates the mechanism, path loss and tissue safety of the state-of-the-art wireless communication methods used in brain neural implants.

The human head is comprised of scalp, skull, dura, cerebrospinal fluid (CSF), gray matter (GM), and white matter, as shown in Figure 1 (a). By using neural implants, three types of electrical potentials in Figure 1 (b) can be recorded: electrocorticogram (ECoG), local field potentials (LFPs), and action potentials (APs or spikes). A typical neural implant architecture is shown in Figure 1 (c), primarily composed of five modules: (1) a recording module for neural signal acquisition, amplification, and digitization; (2) a signal processing module such as data compression; (3) a stimulation module such as optical or electrical stimulation; (4) a wireless communication module to send the recorded data or receive external commands; and (5) a power management module for energy harvesting and voltage regulation. This paper mainly focuses on the communication part.

Recent wireless intra-body communication (IBC) methods for neural implants include far-field radio frequency (RF) [18, 19] , near-field inductive coupling (IC) [20], ultrasonic (US) [21], near-infrared (NIR) [22], capacitive body coupling (CBC) [23], and galvanic body coupling (GBC) [24, 25] . RF communication is the most widely used data telemetry method due to its mature technology and long-distance transmission [26]. IC technology, which employs magnetic field induction between coils, is commonly utilized in wireless short-distance power and data transfer [27]. US transmits information via mechanical waves at frequencies exceeding 20 kHz, which has been a promising method due to its low attenuation in tissue [28]. NIR data is sent by small light-emitting diodes (LEDs), enabling the design of sub-mm implants [29]. CBC and GBC are both types of body channel communication (BCC), in which signals are sent using the human body as a conductive medium [30]. CBC creates a stimulated electric field around and through the human body, while GBC injects a weak current into human tissue.

To better comprehend neural implants from the perspective of wireless communication, this paper first introduces communication requirements in Section 2. Several wireless intra-body communication methods are discussed in the transmission mechanism, path loss, and tissue safety in Section 3. The challenges and optimizations for these neural interfaces are summarized in Section 4. Section 5 concludes the paper.

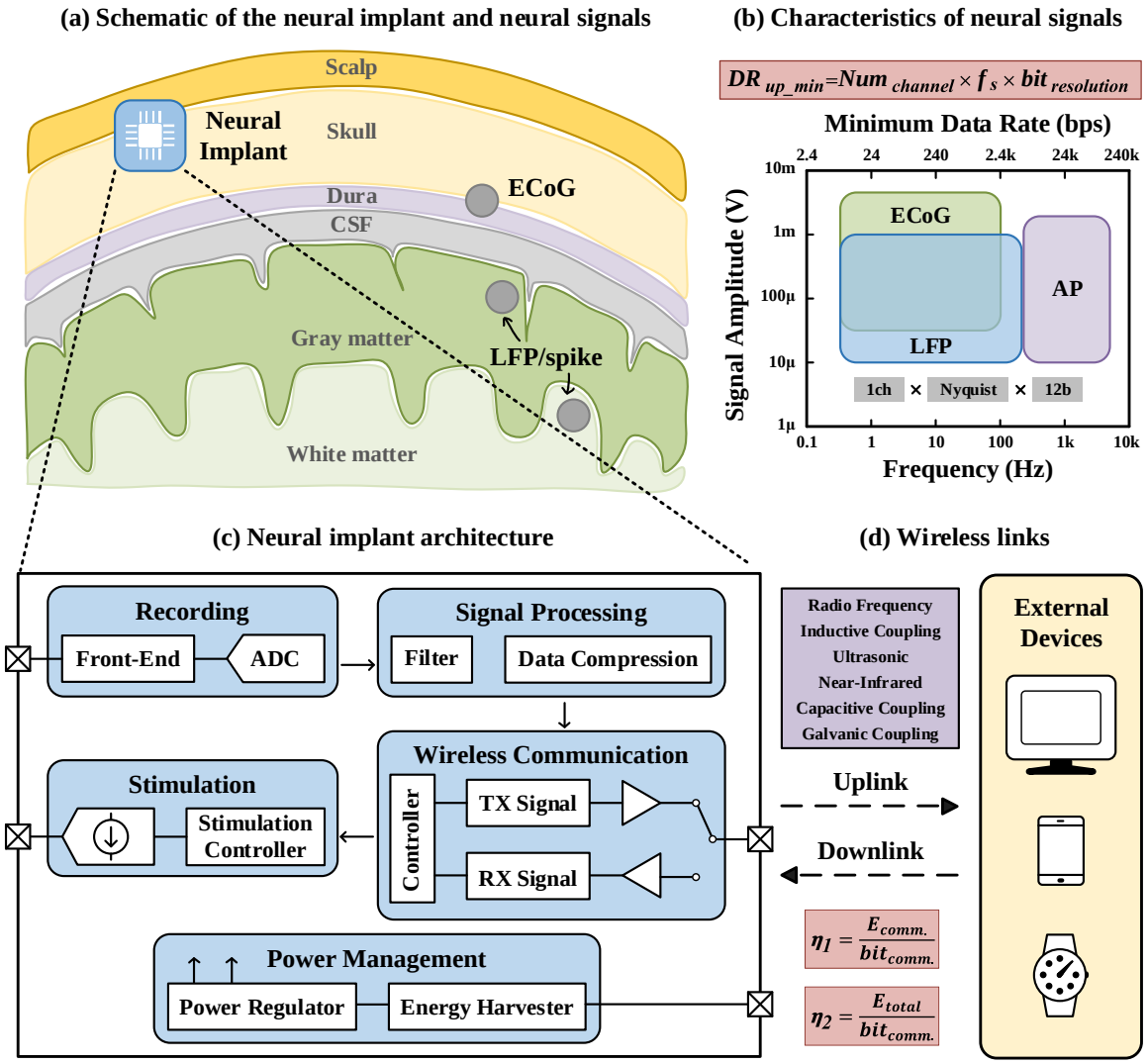

Figure 1. (a) Schematic of the neural implant and neural signals. (b) The signal amplitude, frequency range, and data rate of neural signals. The minimum uplink data rate is derived by using one recording channel, the Nyquist sampling theorem, and a 12-bit resolution. (c) Neural implant architecture includes a recording module, a signal processing module, a stimulation module, a wireless communication module, and a power management module. (d) Wireless links between the neural implant and external devices.

2. Communication requirements

In this section, the main communication requirements for neural implants are briefly introduced.

Uplink and downlink: As shown in Figure 1 (d), wireless communication transmission includes both uplink and downlink channels. The implant transmits the collected signals to external devices via the uplink, while external devices send configuration information and control commands to the implant via the downlink. In general, the uplink requires a significantly greater transmission rate than the downlink since the amount of data acquired for neural signals is rather considerable. Recording systems require a one-way uplink connection, whereas stimulators only need a downlink channel. Combining recording and stimulation, it is usually called a closed-loop brain-computer interface. Since uplink has higher communication requirements, this study focuses on both recording and closed-loop devices for the purpose of comparing the performance of each communication technique.

Data rate: Uplink data rate requirements are primarily determined by the number of

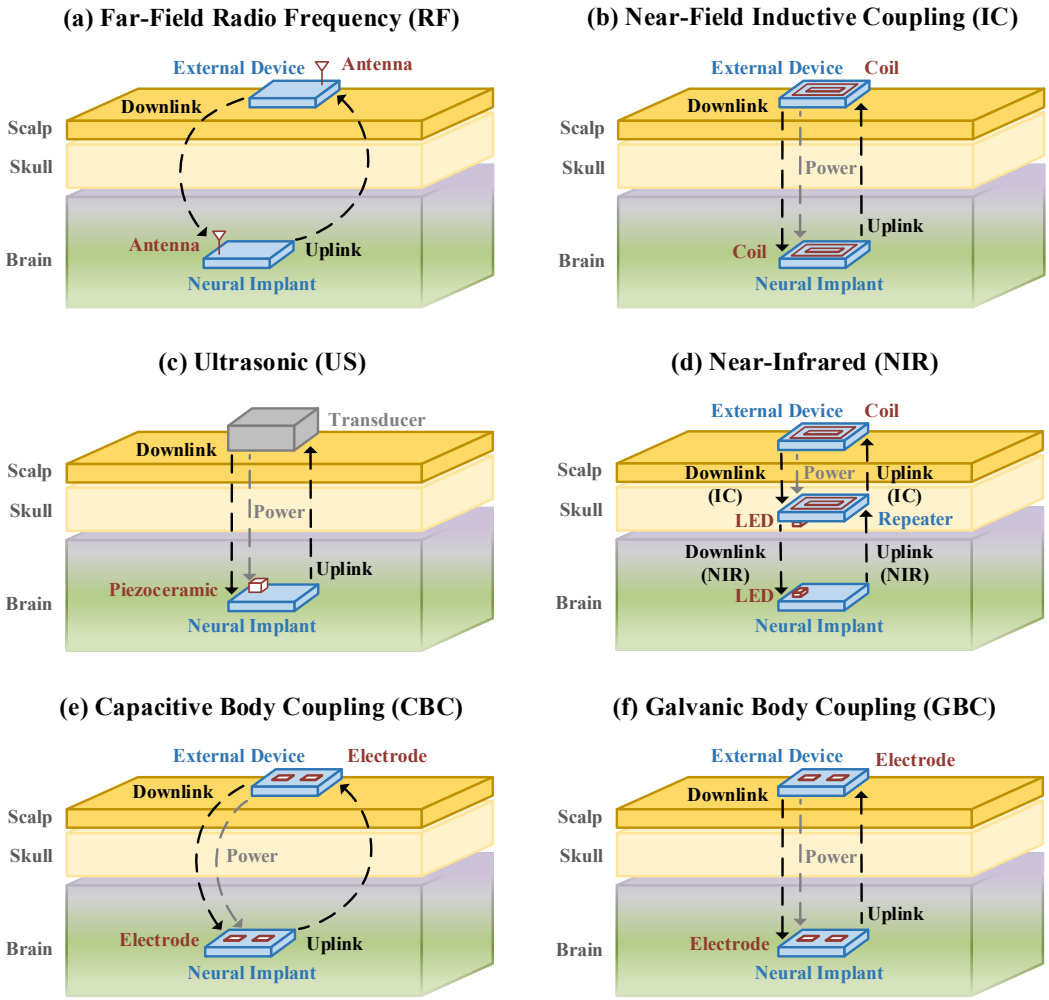

Figure 2. Wireless intra-body communication methods.

recording channels ($Num_{channel}$), sampling frequency (f_s), and collecting module resolution ($bit_{resolution}$). The minimum uplink data rate (DR_{up_min}) can be calculated as follows:

$$DR_{up\_min} = Num_{channel} \times f_s \times bit_{resolution} \tag{1}$$

The sampling frequency for various neural signals is different. As shown in Figure 1 (b), ECoGs and LFPs have frequencies less than 400 Hz, while APs have frequencies ranging from 400 Hz to 7kHz. In order to restore the original signal without distortion, the Nyquist sampling theorem states that the sampling frequency must be at least twice the maximum frequency contained in the original signal. Assuming that the resolution of ADC is 12 bits, the calculated data rate of a single recording channel is displayed in Figure 1 (b). It is obvious that APs require a higher data rate than ECoGs and LFPs.

Energy efficiency: Since power consumption is proportional to data rate, it is not intuitive to estimate the performance of different wireless communication devices only by power consumption or data rate. Therefore, the energy per bit (η_1) is commonly used for performance comparison:

$$\eta_1 = \frac{E_{comm.}}{bit_{comm.}} \tag{2}$$

Theoretically, the communication energy ($E_{comm.}$) should be utilized to calculate the energy efficiency with the data rate ($bit_{comm.}$) mentioned above. However, as the communication energy is typically unknown in most reported implants, the total energy (E_{total}) is adopted

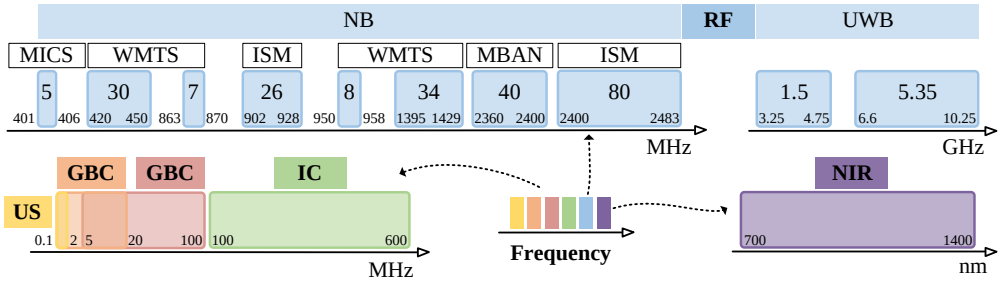

Figure 3. Frequency bands of intra-body communication methods.

instead, as shown below:

$$\eta_2 = \frac{E_{total}}{bit_{comm.}} \tag{3}$$

As a result, there will be some variance in the η estimate. Reducing η is crucial for improving energy efficiency.

3. Wireless intra-body communication

This section discusses the mechanism, path loss in tissue and brain, and tissue safety of the above-mentioned wireless technologies.

3.1. Mechanism

Far-field radio frequency communication employs antennas for long-distance (0.01-10 m) information transmission, as shown in Figure 2 (a). Electromagnetic waves are utilized in the form of narrowband (NB) or ultra-wideband (UWB) signals. NB operates on frequency bands such as Medical Implant Communications Service (MICS), Wireless Medical Telemetry Service (WMTS), Medical Body Area Network (MBAN), and Industry, Scientific, and Medical (ISM) [31], as shown in Figure 3. UWB transmits signals at a high data rate in the wide frequency range of 3.1-10.6 GHz.

The RF frequency is an important consideration and trade-off. As the frequency increases, the size of the antenna can be small enough for brain implantation [32]. However, the penetration depth also decreases as the path loss within tissue layers increases severely. Meanwhile, it is obvious that increasing RF frequency leads to higher power consumption [18], which is unfavorable for brain tissue safety.

Mature commercial protocols have led to the widespread use of NB communication in brain implants, such as Bluetooth [33–35] , Zarlink [36] and Zigbee [37]. These commercial off-the-shelf (COTS) components allow for low-cost and simple system implementation but are substantial in size. A wireless neural recording device based on Bluetooth low-energy (BLE) in [33] achieves high-quality signal recordings and a 5-meter transmission range, weighing <3.9 g and measuring $15\times15\times12$ mm^3. With a diameter of 50 mm, a 64-channel ECoG recording implant employs a Zarlink radio chip (ZL70102, MicroSemi) in the 402-405 MHz MICS band to realize a transmission rate of up to 450 kbps across a distance of up to 2 meters [36].

Besides using COTS components, SoC is commonly used in implantable devices, which typically involves antennas [18, 38, 39] or coils [40, 41] . An antenna as a surface-mounted device (SMD) in [18] is utilized for a 2.4/3.2 GHz dual-band OOK transmission at 54 Mbps with a range of up to 4 meters, at the cost of an incomplete implanted bulky size. The uplink telemetry in [38] sends a 6.78 Mbps data stream using on-off keying (OOK) modulation of a 434 MHz RF carrier via a 6 cm monopole antenna. At the expense of transmission distance, the work in [41] employs the OOK oscillator's on-chip coil as a transmitting antenna to send data for miniaturization at a carrier frequency of 600 MHz.

In addition to the widely used NB communication, UWB is a resurrected wireless telemetry technology that offers the benefits of wide bandwidth and high energy efficiency. Two UWB transmitters in [39] are used by a wireless closed-loop neurostimulator to communicate with receivers located 0.1-2 m apart at data rates ranging from 10-46 Mbps. At a center frequency of 4 GHz, a 65536-channel recording and stimulating microelectrode array SoC employs an impulse radio UWB (IR-UWB) transmitter to reach a data rate of 108 Mbps with 50 pJ/bit [19].

Near-field inductive coupling technology allows for short-distance (1-3 cm) communication and power transmission using magnetic field induction between coils, as shown in Figure 2 (b). When it comes to communication performance and power efficiency, careful consideration should be given to coil alignments, size, and quality factors. Misalignment can significantly increase the communication bit error rate (BER) [42] and reduce power delivery efficiency [43]. With increasing coil size, the operating range and power transmission will be improved [42]. However, it will also make miniaturization of neural implants more difficult. High-quality factor enables a high power transfer efficiency (PTE) [44] at the expense of a restricted data rate.

IC was initially utilized for wireless power transfer before being gradually extended to wireless communication in recent years. In general, inductive coupling in neural implants provides both wireless power and data telemetry. It may be implemented in various configurations, including two dedicated inductive links [45], a single pair of coils [46–48] , and an extra resonator [43, 49, 50] . Using two separate inductive links with two pairs of coils allows for a high data rate of 3 Mbps while maintaining a high PTE, but it requires a large size [51]. To minimize device size for implantation, only one pair of coils at 13.56 MHz is chosen to deliver both power and data, typically with a backscatter uplink to save power [46, 47] . However, this approach suffers from an inconsistency between efficient power transfer and high data rates. For example, [46] has a high PTE of 48% but a low data rate of 105 kbps, while [47] has a high data rate of 1 Mbps but a poor PTE of 10-15%. In particular, a novel structure with an additional resonator is proposed to power distributed implants [43], allowing for implants downsizing with a tiny coil [50].

Ultrasound waves are mechanical waves with frequencies exceeding 20 kHz, which can effectively propagate in media composed mainly of water. Similarly, since the human body is composed for 65% of water, ultrasonic intra-body communication [52] and power transfer becomes a novel solution for implanted devices. As shown in Figure 2 (c), ultrasonic transducers are necessary for the conversion between ultrasound and electrical signals, with strict orientation constraints owing to piezoelectric crystals. The selection of ultrasonic frequency requires a balance between data rate and intra-body transmission distance. Lower frequency allows for deeper implantation and a higher SNR, but at a limited data rate [28].

Compared with neural stimulators [53, 54] , there are fewer neural recording implants [21, 55] using ultrasonic communication due to its high skull absorption and low data rate. [55] demonstrates the first battery-free ultrasonic backscattering neural recording system with a data rate of 0.5 Mbps at 1.85 MHz. Besides, [21] presents a 0.8 mm^3 neural implant with ultrasonic powering and data telemetry, consisting of a 0.25 mm^2 recording integrated circuit (IC), a single piezoceramic resonator, and two recording electrodes. To reach a data rate of more than 35 kbps, uplink data is transmitted using analog amplitude modulation with a main carrier frequency of 1.78 MHz.

Near-infrared technology uses LEDs for data modulation and demodulation to transmit communication signals, which is beneficial for the design of micro-implants. However, due to considerable scattering and absorption losses, the optical wireless link has a very short transmission range (< 5 mm). Therefore, a large sub-cranial repeater is required for NIR communication to work with the inductive link to form a two-step neural recording system [22], as shown in Figure 2 (d). Furthermore, alignment and light-sensitive parasitic short-circuit currents might have an impact on overall performance [56].

In view of the small form factor, implantable recorders with optical power and data transfer have been proposed as a potential solution to collect neural signals with minimal tissue damage. In 2019, [57] presented a ten-channel neural acquisition system with inductive coupling power transfer and NIR uplink data telemetry, reaching a high data rate of 3 Mbps. However, it weighs 3.9 g and measures 3.4 cm^3 due to its power coil. Furthermore, with a partly transparent encapsulation that exposes the NIR-LED to light for NIR communication, the light-sensitive parasitic short-circuit currents problem should be carefully considered. To address these challenges, [56] introduced a light-tolerant neural recorder capable of functioning at up to 300 $\mu W/mm^2$ of light exposure, using optical power and data telemetry via a customized photovoltaic and micro-LED. The work in [58] achieves the smallest size of $250\mu m \times 57\mu m$ by employing a heterogeneously integrated AIGaAs that works as both a photovoltaic and light-emitting diode.

Capacitive body coupling communication transmits signals by generating a stimulated electric field through signal electrodes, ground electrodes, the human body and the Earth ground, as shown in Figure 2 (e). The signal electrodes make direct contact with the body *in vitro* [59] or *in vivo* [60] using conductive materials such as copper, gold, and platinum to construct a low-loss forward path. As a result, CBC can facilitate long-distance (< 2 m) wireless links and cover the entire body [23]. The outside ground electrode simply floats using the same conductive materials as the signal electrodes, while the inside one employs insulating materials to insulate from the body [61]. Then, the backward path is composed of the coupling between TX and RX ground electrodes, as well as the coupling between TX/RX ground electrode, the human body and the Earth ground. For this reason, CBC is vulnerable to disturbance in the surroundings [62].

Recently, implanted devices have used CBC to obtain a high data rate while minimizing tissue absorption. In 2022, [23] proposed the first and only neural implant with capacitive coupling data transmission and power delivery, validated through *in vivo* recordings on rats. The implant can transmit the recorded four-channel ECoG signals to an external device placed on the back of the rat, with a data rate of 20.48 Mbps and a low power consumption of 644 μW. The external BCC RX recovers the received data and then sends them to a computer via Bluetooth.

The galvanic coupling body channel communication injects a weak current into human tissue using pairs of conductive differential electrodes for wireless transmission, as shown in Figure 2 (f). Since the signal is mostly transmitted within the human body, both the forward and backward channels of GBC have little loss [63]. Besides, unlike CBC, it is independent of external environmental interference. However, GBC suffers from a restricted communication distance due to the self-cancellation of the close-range differential electrodes [64].

GBC is a feasible approach for implants with the advantages of low propagation loss and frequency. [65] proposed Bi-Phasic Quasi-static Brain Communication (BP-QBC) in a neural implant SoC. By adding a DC-blocking capacitor on the base of GBC, BP-QBC can eliminate the DC power entering into the tissue to achieve a low power consumption of less than 1 μW. The work in [25] introduced passive galvanic coupling for neural recording. The body tissue is used to establish a galvanic loop for power delivery, while the recorded data of the implant adjust the loop current to provide passive communication with minimal power dissipation. Unlike inductive coupling backscatter communication, passive GBC employs miniature electrodes instead of bulky coils, leading to a smaller size of 5.9 mm^3. However, the data rate of 250 kbps is insufficient to record multiple-channel APs simultaneously.

3.2. Path loss in tissue and brain

In the two-port network, the path loss (PL) is generally defined as the ratio of transmitted power at port 1 (P_{TX}) to received power at port 2 (P_{RX}) as shown in Equation (4). When the input impedance of two ports is 50Ω, PL can be defined in terms of the scattering parameter (S_{21}),

Table 2. Path Loss in Tissue

Method	Tissue	Depth	Frequency/ Wavelength	Min. Attenuation	Max. Attenuation
RF [67]	Skin @ Stimulation	1cm	100-700 MHz	64dB @ 420MHz	106dB @ 250MHz
RF [67]	Skin @ Stimulation	1cm	0.4-3 GHz	60dB @ 2.75GHz	98dB @ 0.9GHz
RF [67]	Skin @ Stimulation	1cm	1-12 GHz	52dB @ 1.4 GHz	122dB @ 11.2GHx
IC [68]	Arm @ Stimulation	2.5-8cm	402-405 MHz	60dB @ 2.5cm	75dB @ 8cm
US [69]	Tissue @ Water	1-36cm	320 kHz	100dB @ 1cm	156dB @ 36cm
NIR [70]	Skin @ Stimulation	0.5cm	400-1000 nm	400dB @ 1000nm	2000dB @ 400nm
CBC [23]	**Tissue @ Pork**	5cm	0.01-300 MHz	26dB @ 20MHz	40dB @ 0.01MHz
GBC [25]	**Skin & Fat & Muscle @ Pork**	2.5cm	0.1-20 MHz	32dB @ 3MHz	39dB @ 0.1MHz

0-40dB | 40-80dB | 80-120dB | 120-160dB | >160dB

Table 3. Path Loss in Brain

Method	Tissue	Depth	Frequency/ Wavelength	Min. Attenuation	Max. Attenuation
RF [71]	Brain @ Stimulation	0-1.1cm	2.5 GHz	20dB @ 0.1cm	51dB @ 1.1cm
RF [71]	Brain @ Stimulation	0-1.1cm	12 GHz	28dB @ 0.1cm	76dB @ 1.1cm
IC [72]	**Piglet head**	2-6cm	406 MHz	43dB @ 2cm	56dB @ 6cm
US [73]	**Human skull**	1cm	0.3-1.7 MHz	8dB @ 0.3MHz	58dB @ 1.7MHz
NIR [70]	Brain @ Stimulation	0.5cm	400-1000 nm	100dB @ 1000nm	500dB @ 400nm
CBC [74]	**Rat brain**	0.2cm	10-375 MHz	25dB @ 200MHz	40dB @ 10MHz
GBC [25]	Skull @ Pork	2.5cm	0.1-20 MHz	36dB @ 1MHz	43dB @ 20MHz
GBC [65]	human brain @ PBS [a]	0.1-6cm	1MHz	10dB @ 0.1cm	55dB @ 6cm
GBC [65]	**Mouse brain**	0.1-1cm	1MHz	10dB @ 0.1cm	32dB @ 1cm

[a] Phosphate-buffered saline.

0-20-40 | 40-80dB | 80-120dB | 120-160dB | >160dB

which is the forward transmission coefficient from port 1 to port 2 [66]. By utilizing vector network analyzer (VNA) to obtain the (S_{21}), the path loss in dB can be easily determined as Equation (5).

$$PL = \frac{P_{TX}}{P_{RX}} = \frac{1}{|S_{21}|^2} \tag{4}$$

$$PL_{dB} = 10\log_{10}\frac{1}{|S_{21}|^2} = -10\log_{10}|S_{21}|^2 = -20\log_{10}|S_{21}| = -|S_{21}|_{dB} \tag{5}$$

The path loss of different wireless intra-body communication methods in tissue is listed in Table 2. The work in [67] evaluated the path loss of RF communication inside the human body with a depth of 1 cm by simulations. The PL is in the 50–120 dB range at the frequency bands of 100–700 MHz, 0.4–3 GHz, and 1–12 GHz. [68] reported the path loss as a function of the distance between the forearm implanted antenna and the external antenna. The path loss generally increases with distance. It has a maximum value of less than 80 dB and a minimum of about 60 dB. The 320 kHz ultrasonic communication link is characterized at different depths in a large water tank that mimic the human tissue environment [69]. Though the acoustic attenuation in tissue is low, the loss of energy conversion is high. For this reason, the lowest US path loss is 100 dB at 1 cm depth. A complete path loss model of optical wireless communication in biomedical applications is formulated in [70]. The minimal path loss with a transmission wavelength of 1000 nm at a depth of 0.5 cm in skin tissue is 400 dB, which is excessively more than the path loss for other techniques. Pork is usually used to measure the channel characteristics of body communication technologies [23] [25]. It is shown that CBC and GBC have the path loss between 25 and 40 dB, which is significantly less than that of other methods.

Given that the brain is one of the most complex organs in the body, it is essential to investigate the brain channel models of various telemetry technologies to develop better applications. Table 3 lists the path loss in the brain. In [71] and [32], finite element method (FEM) stimulation was used to study the path loss along brain layers at different frequencies. It is demonstrated that the scalp and CSF layers, with their high conductivity to permittivity ratio, are where the majority of the loss is happening. A near-field communication link was tested in a CSF phantom and pig primate in [72]. For a distance covering from 2 to 6 cm at 406 MHz, the established PL model yields an attenuation between 43 and 56 dB. The work in [73] measured the acoustical characteristics of many fresh and subsequently formalin-immersed human skulls. Over the frequency range of 0.3-1.7 MHz, the reflection loss varies from about 3-15 dB, whereas the insertion loss ranges from about 8-58 dB. [70] showed that as the transmitted optical radiation's wavelength increases, the brain path loss decreases. Typically, *in vivo* capacitive [74] or galvanic [65] coupling body channel characteristics are measured in the brain of an anesthetized rat, with a path loss of less than 40 dB. Pork [25] or phosphate-buffered saline (PBS) [65] are the two most common settings used for *in vitro* brain channel measurements.

The majority of path loss models are derived through simulation as opposed to actual measurements due to practical and ethical concerns. Using various measuring configurations will probably result in a different path loss. For example, lower measured PL may arise from insufficient ground isolation between the TX and the RX in CBC communication [75]. Therefore, the path loss listed in Table 2 and Table 3 may only be used as a simple comparison.

3.3. Tissue safety

The impact of different fields and waveform types used in wireless communication methods on brain tissue should be carefully considered. However, there is still a lack of guidelines and limitations to prevent the adverse health effects of neural implants in humans.

In order to verify the tissue safety of neural implants, IEEE Standard C95.1 [76, 77] and other guidelines [78] are employed as references regarding exposure restrictions in electric, magnetic, and electromagnetic fields. The specific absorption rate (SAR, W/kg) refers to energy absorbed within a specified mass range. Compared with whole-body exposure, local exposure to the head is more appropriate for brain neural implants, with an allowable SAR of 2 W/kg [77].

The ultrasonic communication limit is characterized by intensity (mW/cm^2), which is the power transferred in the direction of acoustic wave propagation. The spatial-peak temporal-average intensity (I_{SPTA}) of ultrasonic is limited to be 720 mW/cm^2 by the Food and Drug Administration (FDA) [79]. Furthermore, fluctuating pressure of an acoustic field may result in the expansion and contraction of gas bubbles, known as cavitation [16]. This phenomenon should also be taken into account when assessing the potential health effects of ultrasonic communication.

It is important to carefully analyze the possibility of tissue overheating during NIR transmission. The ISO 14708-1:2000 E standard requires that heat accumulation be limited to a temperature rise of no more than 2 ℃. According to [80], a 1 mm^2 area continuously illuminated by NIR lasers increases the peak temperature by around $1.8℃/100mW$. Continuous illumination over 250 mW causes lasting harm.

3.4. Performance summary

From Table 4, it is obvious that no specific implant outperforms the others in all performance metrics. Each wireless intra-brain communication method has benefits and downsides; hence, it is often chosen depending on the specific application needs.

Comparing RF communication to other technologies, the data rates are significantly higher,

Table 4. Comparison of the Neural Implants

		TCASII'20 [18]	VLSI'23 [19]	ISSCC'24 [20]	JSSC'19 [21]	ISSCC'20 [22]	JSSC'22 [23]	ESSCIRC'22 [24]
CMOS Process [nm]		65	130	180	65	180	110	65
Chip Size [mm^2]		3.72×3.68=13.7	144	1.5×1=1.5	0.5×0.5=0.25	0.19×0.17=0.0323	2.8×1.4=3.92≈4	1×1=1
Implant Volume [mm^3]		1900×1800×U/K	144×0.025=3.6	4×4×2.5=40	0.8	~0.00323 [a]	~32 [a]	5.45
Implant Weight [mg]		1700	U/K	18	U/K	U/K	U/K	20
Component [e]	Communication	1 Antenna	1 Antenna	1 Coil [b]	1 Piezoceramic [b]	1 LED	1 Electrode	Electrode [c]
	Power	1 Coil	1 Coil	1 Coil [b]	1 Piezoceramic [b]	1 Photovoltaic	1 Electrode	Electrode [c]
	Off-chip [d]	1 Antenna, 1 Coil, 1 Oscillator etc.	None	1 Capacitor, 1 Coil	1 Piezoceramic	1 LED, 1 Photovoltaic	2 Electrodes	1 Capacitor, Electrode [c]
Sub-Cranial Resonator/Repeater/Relay		None	None	1 Resonator coil	None [f]	1 Repeater	None	None
Recording	Channel Number	64	65536 [k]	1	1	1	4	16
	Neural Signal	AP	LFP	LFP	AP	AP	ECoG	U/K
Stimulation		No	Yes	Yes	No	No	No	Yes
Uplink	Data Link	RF-NB	RF-UWB	Inductive	Ultrasonic	NIR	CBC	GBC
	Frequency [Hz]	2.4/3.2 G	4 G	144 M	1.78 M	8 k	40.96 M	U/K
	Data Rate [bit/s]	54 M	108 M	U/K	>35 k	100 [a]	20.48 M	800 k [g]
	Energy Per Bit [pJ/bit] (paper)	44/48	50	U/K	U/K	6.7 [h]	32	13.2 [g]
	Energy Per Bit [pJ/bit] (η1)	44/48	N/A	N/A	N/A	~2300	~18.87	0.6125 [g]
	Energy Per Bit [pJ/bit] (η2)	48/52	~359	N/A	~1077	~7400	~31.45	2.25 [g]
	Bit Error Rate	$\sim10^{-6}$	U/K	U/K	U/K	U/K	$\sim10^{-4}$	$\sim10^{-3}$
Downlink	Data Link	N/A	RF-UWB	Inductive	N/A	NIR	N/A	GBC
	Data Rate [bit/s]	N/A	54 M	U/K	N/A	U/K	N/A	1 k
Power Link		Inductive	Inductive	Inductive	Ultrasonic	NIR	CBC	GBC
TX-RX	Implant Depth [cm]	U/K	U/K	U/K	4.5~6	U/K	~0.5	U/K
	Transmission Distance [cm]	400	U/K	U/K	4.5~6	U/K	10	U/K
	Alignment [i]	Not Required	Not Required	Required	Required	Required	Not required	Required
Power	Total [μW]	2570/2810	38800	270 [j]	37.7	0.74	644	1.8
	Uplink [μW]	2370/2610	5400 [a]	U/K	U/K	0.23 [a]	386.4 [a]	0.49
In Vivo	Validation	Yes	Yes	Yes	No	Yes	Yes	Yes
	Fully Implanted	No	Yes	Yes	No	U/K	Yes	Yes

N/A: Not available U/K: Unknown

Best | Worst | Can not compare

[a] Estimate based on the original paper.
[b] The same component used for communication and power supply.
[c] Unknown number.
[d] Exclude the commonly required off-chip components for neural recording and stimulation. (e.g. electrodes, LEDs)
[e] Consider the implant only.
[f] In vitro validation may not need relays, but in the brain, where considerable loss occurs after passing through the skull, relays are necessary.
[g] Digitization happens at Hub RX.
[h] Post layout stimulation.
[i] Consider communication only.
[j] Measured at maximum stimulation current.
[k] With 4 to 1 electrode multiplexing. Only 1024 channels can be sampled simultaneously.

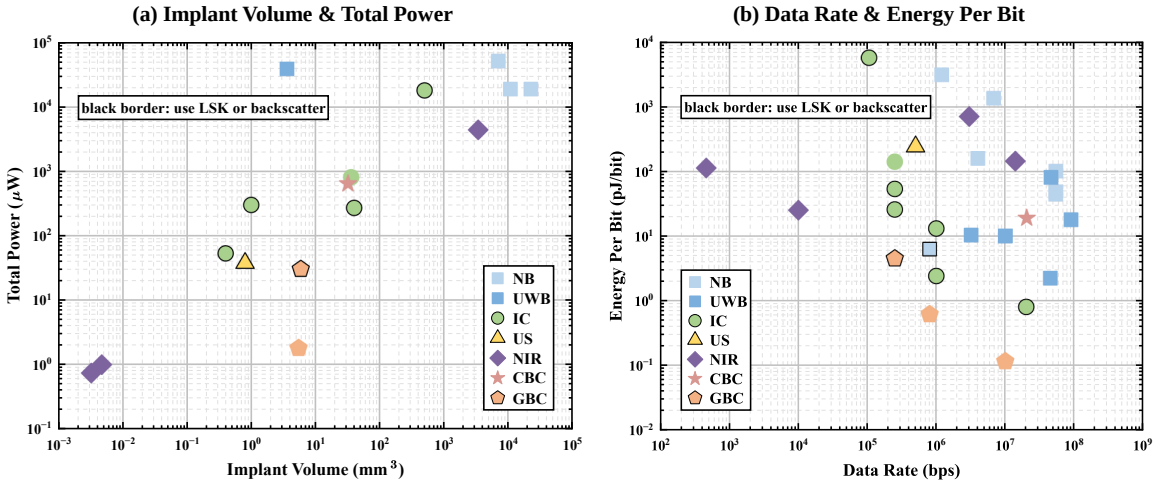

Figure 4. Compare neural implants using different intra-body communication techniques. (a) Total power vs implant volume. (b) Energy per bit vs data rate.

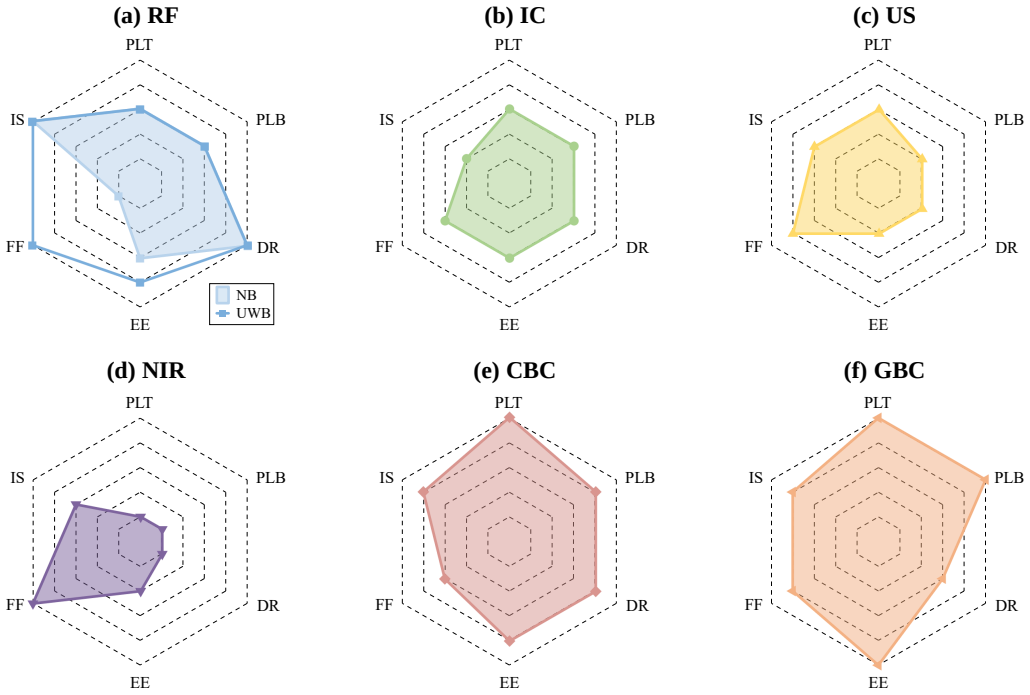

PLT: path loss in tissue; PLB: path loss in brain; DR: data rate
EE: energy efficiency; FF: form factor of the device; IS: interference susceptibility
Note: points away from the center represent better performance

Figure 5. Qualitative comparison of intra-body communication methods.

which allows for simultaneous transmission of high-density neural recordings [18, 19] . In the early stages of implantable electronics, NB was the most widely employed wireless telemetry technique because of its low BER, high data rate, and long-distance transmission. However, the presence of off-chip components such as an antenna and an oscillator renders it too large and heavy to be fully implanted into the brain. In contrast to NB, the development of UWB technology in micro neural implants has received more attention since it can deliver great data throughput with compact on-chip antennas. The most current UWB transceivers can achieve data rates of several Gbps and energy efficiency of a few pJ/bit [81, 82]. If these techniques can be used to high-throughput neural interfaces without sacrificing performance, it will represent a significant step forward in the development of neural implants.

Compared with RF, the merits and demerits of the inductive coupling implant [20] are not very obvious. On the one hand, using coils as power and data telemetry antennas enables a smaller implant volume with a lower carrier frequency and thus lower power consumption. On the other hand, inductive coupling has a relatively low data rate ([45] 3 Mbps, [46] 105 kbps) and requires alignment.

The implants employed ultrasonic [21] or NIR [22] technology to reach sub-mm size, which is ideal for brain implantation with minimal tissue damage. However, the two communication methods suffer from significant loss owing to dispersion and skull absorption. For this reason, a sub-cranial repeater or relay is required. Furthermore, the lowest data rate and alignment requirement limit their use in multi-channel recording or distributed free-floating implants.

In general, the implants that use BCC [23–25] provide the best overall performance. The power required to transmit each bit across a low-loss human medium can be very low, allowing BCC to transfer data rates higher than other wireless technologies within the same power budget. This significantly reduces the conflict between high data throughput and low power consumption. Without any other sub-cranial components, only tiny and thin electrodes are beneficial to miniaturize size and reduce surgical difficulties.

Figure 4 shows the comparison of neural implants using different intra-body communication techniques. When it comes to implant volume and power consumption, NIR devices are the least and RF devices are the most. From Figure 4 (b), GBC technologies have a relatively high data rate and consume the least energy per bit, whereas UWB methods achieve the highest data rate with relatively high energy efficiency. The integration of load-shift keying (LSK) or backscatter technologies can significantly increase energy efficiency by eliminating the active transmitter in implants [83, 84] . The qualitative comparison of IBC methods are shown in Figure 5. Points away from the center represent better performance. Generally speaking, UWB and BCC communications offer the optimum performance.

4. Challenges and optimizations

From the perspective of wireless communication, this section discusses five design challenges and optimizations for neural implants, including safety standards, high energy efficiency, communication latency, data security, and multi-site network.

Safety standards: There is now a lack of guidelines and regulations to prevent the detrimental effects of brain implants on human health, which undermines the case for the constraints of communication metrics. In order to develop safety standards applicable to neural implants, actual human studies that adhere to practical and ethical constraints are required.

High energy efficiency: High-density neural recordings show great promise in neuroscience research, requiring large amounts of data to be transferred to external devices. This means that a high data rate is necessary, typically resulting in higher power consumption. As a result, wireless links with higher energy efficiency, such as human body communication [85], are preferred. Because they allow for a high data rate while acquiring less power, they greatly reduce total power consumption. However, to meet the demands for ever-higher densities of data, high energy-efficiency technologies still need to be developed.

Communication latency: In the majority of implantable device designs, communication latency is rarely taken into account. For closed-loop implants, low communication latency will greatly improve their performance by reducing the neuromodulation cycle. This indicator needs to be focus and further optimized in the future work of neural implants.

Data security: As implants advance from the experimental to the clinical stages, data security needs to be carefully considered. Physical security is preferred owing to its simplicity and minimal resource needs. When compared to conventional radio frequency techniques, body channel communication confines signals to a small area around the body, significantly lowering the risk of hacking by attackers [86]. Additionally, encrypting the neural data can offer more information security. However, this usually comes with an increase in power consumption. Further consideration needs to be given to how to implement encryption with less power usage.

Multi-site network: To reveal higher-level mechanisms of brain functionalities, multi-site network is required to record or stimulate multiple points in the nervous system using several mm-sized free-floating devices. Two modes of transmission may exist between these micro-implants and the external system: 1) A single micro-implant receives data from other nodes and sends them out; 2) Each of these micro-devices sends out data on its own. How to isolate interference from each other remains to be resolved.

5. Conclusion

This survey begins by introducing the communication requirements for neural implants. Following that, several wireless intra-body communications are examined in terms of mechanism, path loss, tissue safety, and implant application. Based on a thorough investigation and comparison of neural implants employing various data telemetry technologies, ultra-wideband and body channel communication generally provide the best overall performance. With technolog-

ical advancements, the challenges of neural implants will be better addressed for widespread human usage during the next decade.

Appendix

Radio frequency (the broad concept, only used for this part) communication uses electromagnetic waves ranging from around 20 kHz to around 300 GHz to transfer information via antennas [87]. For wireless body area networks, IEEE 802.15.6 standard [31] defines three different physical layers (PHYs): (a) human body communication (HBC) ranging from 5 MHz to 50 MHz; (b) narrowband (NB) including frequency bands such as Medical Implant Communications Service (MICS), Wireless Medical Telemetry Service (WMTS), and Industry, Scientific and Medical (ISM); (c) ultra-wideband (UWB) ranging from 3.1 GHz to 10.6 GHz.

As a general definition, the wavelength (λ) of radio frequency can be calculated by its frequency (f) and the light speed $\left(c \approx 3 \times 10^8 m/s\right)$:

$$\lambda = \frac{c}{f} \tag{6}$$

The space around an antenna is often classified into three regions: (a) the near-field region; (b) the transition zone; (c) the far-field region [88]. For antennas that their maximum dimension (D) is shorter than half of the wavelength of the radiation they emit $\left(D < \frac{\lambda}{2}\right)$, the classification criteria is based on the wavelength and the distance (r) from the radiating source:

$$\text{For } D < \frac{\lambda}{2}\ , \begin{cases} r \ll \lambda\ , & \text{(near-field region)} \\ \lambda < r < 2\lambda\ , & \text{(transition zone)} \\ r \gg 2\lambda\ , & \text{(far-field region)} \end{cases} \tag{7}$$

For antennas physically larger than a half-wavelength of the radiation they emit $\left(D > \frac{\lambda}{2}\right)$, the classification criteria is based on the distance (R), the wavelength, and the antenna's maximum dimension:

$$\text{For } D > \frac{\lambda}{2}\ , \begin{cases} R < 0.62\sqrt{\frac{D^3}{\lambda}}\ , & \text{(near-field region)} \\ R \geq 0.62\sqrt{\frac{D^3}{\lambda}}\ ,\ R < \frac{2D^2}{\lambda}\ , & \text{(transition zone)} \\ R \geq \frac{2D^2}{\lambda}\ , & \text{(far-field region)} \end{cases} \tag{8}$$

The wavelength for frequencies ranging from 1 MHz to 10 GHz is between 300 m and 3 cm. This means that the antennas used in most intra-body radio frequency communication are often shorter than half of the wavelength of the radiation they emit $\left(D < \frac{\lambda}{2}\right)$.

Based on the above-mentioned radio frequency, various assumptions are made to distinguish between far-field radio frequency (RF) and near-field inductive coupling (IC) communication in terms of frequency. In RF, the distance (r) from the radiating source is considered to be 1-20 m, but in IC, it is less than 10 cm. To simplify calculations and be consistent with practical applications, the tissue loss is neglected, and the orders of magnitude of $(\ll)$ and $(\gg)$ are considered to equal 1 (10 times). According to (7), the calculated frequency of RF varies from 300 MHz to 10 GHz, whereas IC ranges from 1-300 MHz. In fact, there are no precise cutoffs between these regions, "300 MHz" is only useful for understanding the frequency differences between RF and IC.

Acknowledgments

This work was supported in part by the National Key Research and Development Program of China with grant number 2021ZD0200400.

Conflicts of interests

The authors declare no competing interests.

Authors contribution

Chuer Lin participated in conceptualization, methodology, formal analysis, investigation, data curation, writing of original draft, review and editing, and visualization. Shengqi Zhu and Cheng Han participated in investigation, data curation, and writing of original draft. Shan Yu and Zhiwei Zhang participated in conceptualization, writing of review and editing, supervision, project administration, and funding acquisition. Jingna Mao participated in conceptualization, methodology, writing of original draft, review and editing, supervision, project administration, and funding acquisition.

References

[1] Mott MC, Gordon JA, Koroshetz WJ. The NIH BRAIN initiative: Advancing neurotechnologies, integrating disciplines. *Plos Bio* 2018, 16(11):e3000066.
[2] Wagner FB, Mignardot JB, Le Goff-Mignardot CG, Demesmaeker R, Komi S, *et al.* Targeted neurotechnology restores walking in humans with spinal cord injury. *Nature* 2018, 563(7729):65–71.
[3] Wu YC, Liao YS, Yeh WH, Liang SF, Shaw FZ. Directions of deep brain stimulation for epilepsy and parkinson's disease. *Front Neurosci-Switz* 2021, 15.
[4] Lopez CM, Andrei A, Mitra S, Welkenhuysen M, Eberle W, *et al.* An implantable 455-active-electrode 52-channel CMOS neural probe. *IEEE J Solid-St Circ* 2014, 49(1):248–261.
[5] Moses DA, Metzger SL, Liu JR, Anumanchipalli GK, Makin JG, *et al.* Neuroprosthesis for decoding speech in a paralyzed person with anarthria. *New Engl J Med* 2021, 385(3):217–227.
[6] Lee B, Jia Y, Mirbozorgi SA, Connolly M, Tong X, *et al.* An inductively-powered wireless neural recording and stimulation system for freely-behaving animals. *IEEE T Biomed Circ S* 2019, 13(2):413–424.
[7] Wang L, Suo Y, Wang J, Wang X, Xue K, *et al.* High-density implantable neural electrodes and chips for massive neural recordings. *Brain-X* 2024, 2(2):e65.
[8] Wu L, Liu A, Ward RK, Wang ZJ, Chen X. Signal processing for brain–computer interfaces: a review and current perspectives. *IEEE Signal Proc Mag* 2023, 40(5):80–91.
[9] Miziev S, Pawlak WA, Howard N. Comparative analysis of energy transfer mechanisms for neural implants. *Front Neurosci-Switz* 2024, 17:1320441.
[10] Zhang M, Zhao Z, Ma Y, Zhang C, Song W, *et al.* Wireless compact neural interface for freely moving animal subjects: a review on wireless neural interface SoC designs. *IEEE Solid-State Circuits Mag* 2023, 15(4):20–29.
[11] Wang L, Liu S, Zhao W, Li J, Zeng H, *et al.* Recent advances in implantable neural interfaces for multimodal electrical neuromodulation. *Adv Healthc Mater* 2024, 13(24):2303316.
[12] Kim H, Rigo B, Wong G, Lee YJ, Yeo WH. Advances in wireless, batteryless, implantable electronics for real-time, continuous physiological monitoring. *Nano-Micro Lett* 2023, 16(1):52.
[13] Nair V, Dalrymple AN, Yu Z, Balakrishnan G, Bettinger CJ, *et al.* Miniature battery-free bioelectronics. *Science* 2023, 382(6671):eabn4732.
[14] Zhang M, Tang Z, Liu X, Van der Spiegel J. Electronic neural interfaces. *Nat Electron* 2020, 3(4):191–200.
[15] Luan L, Robinson JT, Aazhang B, Chi T, Yang K, *et al.* Recent advances in electrical

neural interface engineering: Minimal invasiveness, longevity, and scalability. *Neuron* 2020, 108(2):302–321.

[16] Tomlinson WJ, Banou S, Yu C, Stojanovic M, Chowdhury KR. Comprehensive survey of galvanic coupling and alternative intra-body communication technologies. *IEEE Commun Surv Tut* 2019, 21(2):1145–1164.

[17] Abduljaleel HK, Mutashar S, Gharghan SK. Survey of near-field wireless communication and power transfer for biomedical implants. *Eng Tech J* 2024, 42(8):1080–1103.

[18] Lyu L, Ye D, Xu R, Mu G, Zhao H, *et al.* A fully-integrated 64-channel wireless neural interfacing SoC achieving 110 dB AFE PSRR and supporting 54 Mb/s symbol rate, meter-range wireless data transmission. *IEEE Transactions on Circuits and Systems II: Express Briefs* 2020, 67(5):831–835.

[19] Zeng N, Jung T, Sharma M, Eichler G, Fabbri J, *et al.* A wireless, mechanically flexible, 25μm-thick, 65,536-channel subdural surface recording and stimulating microelectrode array with integrated antennas. In *2023 IEEE Symposium on VLSI Technology and Circuits (VLSI Technology and Circuits)*. 2023, pp. 1–2.

[20] Zhao L, Shi W, Gong Y, Liu X, Li W, *et al.* A miniature neural interface implant with a 95% charging efficiency optical stimulator and an 81.9dB SNDR $\Delta\Sigma$M-based recording frontend. In *2024 IEEE International Solid-State Circuits Conference (ISSCC)*, San Francisco, CA, USA, 2024, pp. 558–560.

[21] Ghanbari MM, Piech DK, Shen K, Faraji Alamouti S, Yalcin C, *et al.* A sub-mm^3 ultrasonic free-floating implant for multi-mote neural recording. *IEEE J Solid-St Circ* 2019, 54(11):3017–3030.

[22] Lim J, Moon E, Barrow M, Nason SR, Patel PR, *et al.* A 0.19×0.17mm ^{2} wireless neural recording IC for motor prediction with near-infrared-based power and data telemetry. In *2020 IEEE International Solid-State Circuits Conference (ISSCC)*, San Francisco, CA, USA, 2020, pp. 416–418.

[23] Lee C, Kim B, Kim J, Lee S, Jeon T, *et al.* A miniaturized wireless neural implant with body-coupled power delivery and data transmission. *IEEE J Solid-St Circ* 2022, 57(11):3212–3227.

[24] Chatterjee B, Kumar KG, Xiao S, Barik G, Jayant K, *et al.* A 1.8μW 5.5mm^3 ADC-less neural implant SoC utilizing 13.2pJ/sample time-domain bi-phasic quasi-static brain communication with direct analog to time conversion. In *ESSCIRC 2022- IEEE 48th European Solid State Circuits Conference (ESSCIRC)*, Milan, Italy, 2022, pp. 209–212.

[25] Shen Y, Yang C, Zhang Y, Wang W, Luo Y, *et al.* A battery-free neural-recording chip achieving 5.5 cm fully-implanted depth by galvanically-switching passive body channel communication. *IEEE J Solid-St Circ* 2024, pp. 1–13.

[26] Kassiri H, Bagheri A, Soltani N, Abdelhalim K, Jafari HM, *et al.* Battery-less tri-band-radio neuro-monitor and responsive neurostimulator for diagnostics and treatment of neurological disorders. *IEEE J Solid-St Circ* 2016, 51(5):1274–1289.

[27] Karimi MJ, Jin M, Zhou Y, Dehollain C, Schmid A. Wirelessly powered and bi-directional data communication system with adaptive conversion chain for multisite biomedical implants over single inductive link. *IEEE T Biomed Circ S* 2024, pp. 1–11.

[28] Jaafar B, Neasham J, Degenaar P. What ultrasound can and cannot do in implantable medical device communications. *IEEE Rev Biomed Eng* 2023, 16:357–370.

[29] Lee S, Cortese AJ, Trexel P, Agger ER, McEuen PL, *et al.* A 330μm×90μm opto-electronically integrated wireless system-on-chip for recording of neural activities. In *2018 IEEE International Solid - State Circuits Conference - (ISSCC)*, San Francisco, CA, 2018, pp. 292–294.

[30] Zhao B, Mao J, Zhao J, Yang H, Lian Y. The role and challenges of body channel communication in wearable flexible electronics. *IEEE T Biomed Circ S* 2020, 14(2):283–296.

[31] IEEE standard for local and metropolitan area networks - part 15.6: Wireless body area networks. *IEEE Std 802.15.6* 2012 .

[32] Zaeimbashi M, Lin H, Dong C, Liang X, Nasrollahpour M, *et al.* NanoNeuroRFID: a wireless implantable device based on magnetoelectric antennas. *IEEE J Electromag Rf* 2019, 3(3):206–215.

[33] Idogawa S, Yamashita K, Sanda R, Numano R, Koida K, *et al.* A lightweight, wireless Bluetooth-low-energy neuronal recording system for mice. *Sensor Actuat B-Chem* 2021, 331:129423.

[34] Reich S, Sporer M, Haas M, Becker J, Schuttler M, *et al.* A high-voltage compliance, 32-channel digitally interfaced neuromodulation system on chip. *IEEE J Solid-St Circ* 2021, 56(8):2476–2487.

[35] Zhou A, Santacruz SR, Johnson BC, Alexandrov G, Moin A, *et al.* A wireless and artefact-free 128-channel neuromodulation device for closed-loop stimulation and recording in non-human primates. *Nat Biomed Eng* 2019, 3(1):15–26.

[36] Mestais CS, Charvet G, Sauter-Starace F, Foerster M, Ratel D, *et al.* WIMAGINE: Wireless 64-channel ECoG recording implant for long term clinical applications. *IEEE T Neur Sys Reh* 2015, 23(1):10–21.

[37] Yun S, Koh CS, Jeong J, Seo J, Ahn SH, *et al.* Remote-controlled fully implantable neural stimulator for freely moving small animal. *Electronics-Switz* 2019, 8(6):706.

[38] Jia Y, Guler U, Lai YP, Gong Y, Weber A, *et al.* A trimodal wireless implantable neural interface system-on-chip. *IEEE T Biomed Circ S* 2020, 14(6):1207–1217.

[39] Kassiri H, Salam MT, Pazhouhandeh MR, Soltani N, Perez Velazquez JL, *et al.* Rail-to-rail-input dual-radio 64-channel closed-loop neurostimulator. *IEEE J Solid-St Circ* 2017, 52(11):2793–2810.

[40] Harrison RR, Watkins PT, Kier RJ, Lovejoy RO, Black DJ, *et al.* A low-power integrated circuit for a wireless 100-electrode neural recording system. *IEEE J Solid-St Circ* 2007, 42(1):123–133.

[41] ElAnsary M, Xu J, Filho JS, Dutta G, Long L, *et al.* Bidirectional peripheral nerve interface with 64 second-order opamp-less $\Delta\Sigma$ adcs and fully integrated wireless power/data transmission. *IEEE J Solid-St Circ* 2021, 56(11):3247–3262.

[42] Yeon P, Mirbozorgi SA, Lim J, Ghovanloo M. Feasibility study on active back telemetry and power transmission through an inductive link for millimeter-sized biomedical implants. *IEEE T Biomed Circ S* 2017, 11(6):1366–1376.

[43] Mirbozorgi SA, Yeon P, Ghovanloo M. Robust wireless power transmission to mm-sized free-floating distributed implants. *IEEE T Biomed Circ S* 2017, 11(3):692–702.

[44] Zargham M, Gulak PG. Fully integrated on-chip coil in 0.13 μm CMOS for wireless power transfer through biological media. *IEEE T Biomed Circ S* 2015, 9(2):259–271.

[45] Rush AD, Troyk PR. A power and data link for a wireless-implanted neural recording system. *IEEE T Bio-Med Eng* 2012, 59(11):3255–3262.

[46] Cheng CH, Tsai PY, Yang TY, Cheng WH, Yen TY, *et al.* A fully integrated 16-channel closed-loop neural-prosthetic CMOS SoC with wireless power and bidirectional data telemetry for real-time efficient human epileptic seizure control. *IEEE J Solid-St Circ* 2018, 53(11):3314–3326.

[47] Hou Y, Zhu Y, Ji X, Richardson AG, Liu X. A wireless sensor-brain interface system for tracking and guiding animal behaviors through closed-loop neuromodulation in water mazes. *IEEE J Solid-St Circ* 2024, 59(4):1093–1109.

[48] Hou Y, Zhu Y, Wu X, Li Y, Lucas T, *et al.* A multi-loop neuromodulation chipset network with frequency-interleaving front-end and explainable AI for memory studies in freely behaving monkeys. In *2024 IEEE International Solid-State Circuits Conference (ISSCC)*, San Francisco, CA, USA, 2024, pp. 548–550.

[49] Yeon P, Bakir MS, Ghovanloo M. Towards a 1.1 mm ^{2} free-floating wireless implantable

neural recording SoC. In *2018 IEEE Custom Integrated Circuits Conference (CICC)*, San Diego, CA, 2018, pp. 1–4.
[50] Lee J, Leung V, Lee AH, Huang J, Asbeck P, *et al.* Neural recording and stimulation using wireless networks of microimplants. *Nat Electron* 2021, 4(8):604–614.
[51] Lo YK, Chang CW, Kuan YC, Culaclii S, Kim B, *et al.* A 176-channel 0.5cm^3 0.7g wireless implant for motor function recovery after spinal cord injury. In *2016 IEEE International Solid-State Circuits Conference (ISSCC)*, San Francisco, CA, USA, 2016 pp. 382–383.
[52] Galluccio L, Melodia T, Palazzo S, Santagati GE. Challenges and implications of using ultrasonic communications in intra-body area networks. In *2012 9th Annual Conference on Wireless On-Demand Network Systems and Services (WONS)*, Courmayeur, Italy, 2012, pp. 182–189.
[53] Wang Q, Zhang Y, Xue H, Zeng Y, Lu G, *et al.* Lead-free dual-frequency ultrasound implants for wireless, biphasic deep brain stimulation. *Nat Commun* 2024, 15(1):4017.
[54] Neimat JS, Bina RW, Koenig SC, Demirors E, Guida R, *et al.* A novel closed-loop electrical brain stimulation device featuring wireless low-energy ultrasound power and communication. *Neuromodulation* 2024 .
[55] Seo D, Neely RM, Shen K, Singhal U, Alon E, *et al.* Wireless recording in the peripheral nervous system with ultrasonic neural dust. *Neuron* 2016, 91(3):529–539.
[56] Lim J, Lee J, Moon E, Barrow M, Atzeni G, *et al.* A light-tolerant wireless neural recording IC for motor prediction with near-infrared-based power and data telemetry. *IEEE J Solid-St Circ* 2022, 57(4):1061–1074.
[57] Ng KA, Yuan C, Rusly A, Do AT, Zhao B, *et al.* A wireless multi-channel peripheral nerve signal acquisition system-on-chip. *IEEE J Solid-St Circ* 2019, 54(8):2266–2280.
[58] Lee S, Cortese AJ, Gandhi AP, Agger ER, McEuen PL, *et al.* A 250 μm × 57 μm microscale opto-electronically transduced electrodes (motes) for neural recording. *IEEE T Biomed Circ S* 2018, 12(6):1256–1266.
[59] Mao J, Yang H, Lian Y, Zhao B. A five-tissue-layer human body communication circuit model tunable to individual characteristics. *IEEE T Biomed Circ S* 2018, 12(2):303–312.
[60] Han C, Yu S, Zhang Z, Mao J. A lumped circuit model for implantable body-coupled channel. In *2024 IEEE International Symposium on Circuits and Systems (ISCAS)*. 2024, pp. 1–5.
[61] Zhang K, Hao Q, Song Y, Wang J, Huang R, *et al.* Modeling and characterization of the implant intra-body communication based on capacitive coupling using a transfer function method. *Sensors-Basel* 2014, 14(1):1740–1756.
[62] Mao J, Yang H, Lian Y, Zhao B. A self-adaptive capacitive compensation technique for body channel communication. *IEEE T Biomed Circ S* 2017, 11(5):1001–1012.
[63] Modak N, Nath M, Chatterjee B, Maity S, Sen S. Bio-physical modeling of galvanic human body communication in electro-quasistatic regime. *IEEE T Bio-Med Eng* 2022, 69(12):3717–3727.
[64] Datta A, Nath M, Chatterjee B, Modak N, Sen S. Channel modeling for physically secure electro-quasistatic in-body to out-of-body communication with galvanic Tx and multimodal Rx. In *2021 IEEE MTT-S International Microwave Symposium (IMS)*. 2021, pp. 116–119.
[65] Chatterjee B, Nath M, Kumar K G, Xiao S, Jayant K, *et al.* Biphasic quasistatic brain communication for energy-efficient wireless neural implants. *Nat Electron* 2023, 6(9):703–716.
[66] Kurup D, Joseph W, Vermeeren G, Martens L. In-body path loss model for homogeneous human tissues. *IEEE T Electromagn C* 2012, 54(3):556–564.
[67] De Santis V, Feliziani M. Intra-body channel characterization of medical implant devices. In *10th International Symposium on Electromagnetic Compatibility*. 2011, pp. 816–819.

[68] Stango A, Yazdandoost KY, Negro F, Farina D. Characterization of in-body to on-body wireless radio frequency link for upper limb prostheses. *Plos One* 2016, 11(10):e0164987.
[69] Jaafar B, Soltan A, Neasham J, Degenaar P. Wireless ultrasonic communication for biomedical injectable implantable device. In *2019 41st Annual International Conference of the IEEE Engineering in Medicine and Biology Society (EMBC)*. 2019, pp. 4024–4027.
[70] Trevlakis SE, Boulogeorgos AAA, Chatzidiamantis ND, Karagiannidis GK. Channel modeling for in-body optical wireless communications. *Telecom* 2022, 3(1):136–149.
[71] Zaeimbashi M, Lin H, Wang Z, Chen H, Emam S, *et al.* NanoNeuroRFID: a low loss brain implantable device based on magnetoelectric antenna. In *2018 IEEE International Microwave Biomedical Conference (IMBioC)*, Philadelphia, PA, USA2018, pp. 205–207.
[72] Manoufali M, Bialkowski K, Mobashsher AT, Mohammed B, Abbosh A. In situ near-field path loss and data communication link for brain implantable medical devices using software-defined radio. *IEEE T Antenn Propag* 2020, 68(9):6787–6799.
[73] Fry FJ, Barger JE. Acoustical properties of the human skull. *J ACOUST SOC AM* 1978, 63(5):1576–1590.
[74] Yuk B, Kim B, Park S, Huh Y, Bae J. An implantable body channel communication system with 3.7-pJ/b reception and 34-pJ/b transmission efficiencies. *IEEE Solid-St Circ L* 2020, 3:50–53.
[75] Maity S, He M, Nath M, Das D, Chatterjee B, *et al.* Bio-physical modeling, characterization, and optimization of electro-quasistatic human body communication. *IEEE T Bio-Med Eng* 2019, 66(6):1791–1802.
[76] IEEE standard for safety levels with respect to human exposure to radio frequency electromagnetic fields, 3 kHz to 300 GHz. *IEEE Std C95.1-2005 (Revision of IEEE Std C95.1-1991)* 2006, pp. 1–238.
[77] IEEE standard for safety levels with respect to human exposure to electric, magnetic, and electromagnetic fields, 0 Hz to 300 GHz. *IEEE Std C95.1-2019 (Revision of IEEE Std C95.1-2005/ Incorporates IEEE Std C95.1-2019/Cor 1-2019)* 2019, pp. 1–312.
[78] Specific Absorption Rate (SAR) for Cellular Telephones. Available: https://www.fcc.gov/general/specific-absorption-rate-sar-cellular-telephones (accessed on 28 July 2024).
[79] International Commission on Non-Ionizing Radiation Protection. ICNIRP guidelines on limits of exposure to laser radiation of wavelengths between 180 nm and 1,000 μm. *Health Physics* 2013, 105(3):271–295.
[80] Podgorski K, Ranganathan G. Brain heating induced by near-infrared lasers during multiphoton microscopy. *J Neurophysiol* 2016, 116(3):1012–1023.
[81] Lei J, Liu X, Song W, Huang H, Ma X, *et al.* Design of a low-power, high-data-rate, and crystal-less all-digital IR-UWB transmitter for high-density neural implants. *IEEE J Solid-St Circ* 2024, 59(7):2159–2170.
[82] Song M, Huang Y, Visser HJ, Romme J, Liu YH. An energy-efficient and high-data-rate IR-UWB transmitter for intracortical neural sensing interfaces. *IEEE J Solid-St Circ* 2022, 57(12):3656–3668.
[83] Yang C, Zhang Z, Zhang L, Zhang Y, Li Z, *et al.* Neural dielet 2.0: a 128-channel 2mm×2mm battery-free neural dielet merging simultaneous multi-channel transmission through multi-carrier orthogonal backscatter. *IEEE T Biomed Circ S* 2024, pp. 1–12.
[84] Rhew HG, Jeong J, Fredenburg JA, Dodani S, Patil PG, *et al.* A fully self-contained logarithmic closed-loop deep brain stimulation SoC with wireless telemetry and wireless power management. *IEEE J Solid-St Circ* 2014, 49(10):2213–2227.
[85] Datta A, Sen S. Invited: Can Wi-R enable perpetual IoB nodes? In *2023 IEEE Biomedical Circuits and Systems Conference (BioCAS)*, Toronto, ON, Canada, 2023, pp. 1–5.
[86] Datta A, Nath M, Chatterjee B, Maity S, Sen S. A quantitative analysis of physical security and path loss with frequency for IBOB channel. *IEEE Microw Wirel Compon Lett* 2022, 32(6):792–795.

[87] Wikipedia: Radio frequency. Available: https://en.wikipedia.org/wiki/Radio_frequency (accessed on 28 July 2024).
[88] Wikipedia: Near and far field. Available: https://en.wikipedia.org/wiki/Near_and_far_field (accessed on 28 July 2024).